FIRE AND MATERIALS
Fire Mater. **23,** 209-216 (1999)

Modelling the Charring Behaviour of Structural Lumber

Peter W. C. Lau[1,*], Robert White[2] and Ineke Van Zeeland[1]

[1] Forintek Canada Corp, 4100 Carleton Technology Training Centre, 1125 Colonel By Drive, Ottawa, Ontario Canada, K1S 5RI
[2] Forest Products Laboratory, Forest Services, USDA, One Gifford Pinchot Drive, Madison, WI 53705, USA

Charring rates for large-section timber based on experimental data have been generally established. The established rates may not be appropriately used for the prediction of failure times of lumber members which are small by comparison. It is questionable whether a constant rate can be safely assumed for lumber members since the rate is likely to increase once the centre-point temperature of the members stats to rise. This paper presents an empirically based model of charring rates for Spruce-Pine-Fir (SPF) Machine-Stress-Rated (MSR) *2 × 4* lumber subject to a constant-temperature exposure of 500°C, on the basis of test results on 55 specimens. In order that the model can be used with reliability analysis, on of the two model parameters was treated as a *Logmormal* random variable to explain variations observed in the charring rates. Furthermore, the model has been extended to permit evaluations for other lumber sizes and under exposures such as ASTM E119 fire conditions. The model was compared with existing models and used to predict char data found in the literature. Copyright © 1999 John Wiley & Sons, Ltd.

INTRODUCTION

When wood is exposed to elevated temperatures, its load-carrying capacity is reduced partly by charring, which is considered to have no strength, and partly by strength degradation of the unburnt region. For tire safety engineering of wood structures, the char behaviour is therefore an important design input. For example, it is used to calculate the residual cross-sectional area in a tension member in which the failure event is determined as a balance between the strength in reserve and the increase in stress of the residual area.[1]

Generally, the charring behaviour of wood can either be characterized by the rate of mass-loss (g/s) or by the rate of advance of the char front along a certain axis or dimension (mm/s). The latter definition has been more widely used, particularly in structural fire. safety design and analysis, because it lends itself readily to the calculation of cross-sectional 'residual area'. Typically, the char front is determined on the basis of a series of temperature measurements using thermocouples embedded to different depths of a wood specimen. The position of the char front is then estimated assuming the interface temperature is approximately 300°C.

Charring rates for large-section timber based on experimental data have been generally established. For example, a charring rate of 0.6 mm/min has been determined for glue-laminated timber of medium-density-softwood subjected to ASTM E 119[2] standard fire exposures. The charring rates established under ASTM E 119, CAN/ULC S101,[3] or ISO 834[4] exposures are quite similar, as all these standards have similar temperature-time curves for their fire exposures. For fire safety design of large-section timber structures, Lie[5] recommended the use of a charring rate of 0.8 mm/min for light, dry wood, 0.6 mm/min for medium-density softwood, and 0.4 mm/min for large-section, moist wood. In Canada, analytical expressions for the fire performance of glue-laminated beams and columns are described in Appendix D-2.11 of the National Building Code of Canada (NBCC). These expressions imply a charring rate of 0.6 mm/min. Swedish Building Code SBN 1976 specifies its charring rate as a function of the *opening factor* of the fire load and recommends a lower-bound limit of 0.6 mm/min and an upper-bound limit of 1.0 mm/min.

It has been questioned whether charring rates established for large-section timber are appropriate for lumbar members[6,7] When wood of 'sufficient' mass and volume is exposed to a standard fire-exposure, the rate of charring at the beginning of the exposure is usually more 'rapid' than the rate noted for the teat. This is because the rate more or less stabilizes to a constant rate after the formation of the first few millimetres of char.[8,9,10] Blackshear and Murty[11] attributed the phenomenon to the formation of a steady state of combustion under constant boundary conditions. While the exclusion of the initial non-linear rate data is a reasonable approach for large-section timber, it may be too liberal for lumber members because the first few millimeters of char represents a significant proportion of the total cross-sectional area. It is questionable whether a constant charring rate can be

*Correspondence to: Dr. P. Lau, Forintek Canada Corp, 4100 Carleton Technology Training Ceatre, 1125 Colonel By Drive, Ottawa, Ontario Canada, K1S SRI.

Contract/grant sponsor: Natural Resources Canada (Canadian Forest Services)
Contract/grant sponsor: Province of British Columbia
Contact/grant sponsor: Province of Alberta
Contract/grant sponsor: Province of Québec
Contract/grant sponsor: Province of Nova Scotia
Contract/grant sponsor: Province of New Brunswick

CCC 0308-0501/98/050209-08$17.50

Receiveed / October 1997
Accepted 9 June 1998

safely assumed, given that the rate is likely to increase once the centre-point temperature of the members starts to rise.

König[7] pointed out that the charring rates assumed by various building codes vary considerably, with values up to as high as 1.0 mm/min. In some codes, higher rates are used to compensate for the loss in strength and modulus of elasticity of the unburnt portion, or to compensate for the loss of section due to the 'round-off' effect at comers. The round-off effect refers to the phenomenon that, when a wood member is exposed to fire all around, the comers tend to char more rapidly because the heat is coming from both sides of the corner. In other words, the charring rates are calibrated to the loss of load carrying capacity. For lumber members, using a calibrated charring rate to account for both the loss of material due to charring and the loss of strength in the unburnt section may prove to be too unreliable. Moreover, the reduction in strength and stiffness of the unburnt portion is not necessarily the same for all grades of lumber because of their wide-ranging strength properties. Under these considerations, the charring rates of such members should be accurately characterized and modeled. In addition, the distributional characteristics of the charring rate will be required if reliability are to be carried out on the safety of these members in fires.

This paper presents an empirically based model of charring rates for Spruce-Pine-Fir (SPF) Machine-Stress-Rated (MSR) *2 × 4* lumber subjected to a constant-temperature exposure of 500°C, on the basis of test results on 55 specimens. One of the two parameters of the model was considered as a *Lognormal* random variable to explain variations in the charring rates.

LITERATURE REVIEW

The rate of charring of wood depends on the kinetics of wood combustion, in addition to the external fire exposure characteristics. Wood combustion is an extremely complicated process involving the evolution of flammable gases and the diffusion of these gases to and away from the burning surface (mass transfer). Furthermore, heat generated from the burning gases and oxidizing char in turn fuels the decomposition process through conduction of heat inward (heat transfer). These two transfer processes, however, are continuously modified by the effects of the combustion. The de-composition products are functions of temperature, wood species and density, while the transfer processes depend on wood species, moisture content, permeability, and other morphological factors. Furthermore, the thermal properties influencing these processes are constantly varying, as is the temperature itself.

Early experimental work by Lawson *et al.*[9], Vorreiter[12], followed by Schaffer[13], and than by White[14,15], led to several similar empirical models for describing the charring of wood. These models have the general form of either

$$\frac{\partial x}{\partial t} = \eta_1 t^n \tag{1}$$

or

$$x = \eta_2 t^n \tag{2}$$

where x is the location of the char-front in the direction of charring, $\partial x/\partial t$ is the instantaneous rate of advance of the char front, t is the time, and h_1 and h_2 are regression constants. The exponents n in Eqn (1) determines whether the rate of charring is increasing ($n > 0$), constant ($n = 0$), or decreasing ($n < 0$) as time increases. Truax[10] and Vorreiter[12] showed that, with Eqn (2), n attained a value of 1, provided the initial non-linear rate data were excluded from the regression. Schaffer[13] and White[14] expressed their data as a time-location model. It has the form of

$$t = \eta_3 x^n \tag{3}$$

Models incorporating additional wood parameters such as permeability, density and moisture content have also been derived from the two basic models. A comparison of these models is given in Table 1.

Limited char data are available on some sawn material. One is that of Norén,[16] who reported cross-sectional residual areas and t_f distribution of 45-mm-thick by 120-mm-wide spruce lumber exposed to ISO 834 fire exposure. The lumber had a mean moisture content of approximately 18.6% and an average relative density of 0.47. Another is Schaffer's ASTM E 119 char data[17] on *2 × 4* Douglas-fir lumbar. Discussions concerning Norén's and Schaffer's data are given in the latter part of this paper.

EXPERIMENTAL WORK

The experimental work was carried out at the USDA Forest Products Laboratory in Madison, WI. Sixty specimens of *2 × 4* SPF MSR lumber (35 × 85 mm) of 4880mm (16-foot) length were individually placed in a furnace and exposed to a 'constant' furnace temperature of 500°C and a constant tensile load of 15570 N (3500 lb) until the specimen failed. The interior dimensions of the furnace were 991 mm wide, 1829 mm long, and 1219 mm high (39 in × 72 in × 48 in). It was lined with mineral fibre blankets and heated by eight natural gas burners that maintained the furnace to within ± 10% of any desired temperature. Orientation of the specimens was such that the wider sides were vertical. The length of specimen exposed to the high temperature was 1.8 m. The temperature of exposure was selected to be 500°C so that both charring and strength degradation in the inner portion of the specimens would play an 'equal' role in affecting the time to failure of the specimens.

The tensile load applied was approximately one third of the fifth percentile of the tension capacity of the specimens. Prior to testing, the initial weight and moisture content of each specimen was determined. During testing, the time until failure of the specimen was recorded. Immediately after failure, the specimens were removed from the furnace and cooled with water spray. A 25-mm-thick cross-section was taken from each specimen approximately 600 mm from the centre of the specimen. The samples were subsequently used for the determination of the residual area at the time of failure of the specimen using image analysis. The initial relative density of the specimens had a mean value of 0.51 at test

Table 1. Empirical charring models for some common softwood wood species

Lawson *et al.*[9] Spruce timber beams 38 to 50 mm thick exposed to ASTM E 119; moisture content 12%.	$\frac{\partial x}{\partial t} = 1.041\, t^{-0.2}$ where x = location of char front, mm; t = time, min.
Vorreiter[12] Dried spruce plates 10 mm thick placed horizontally and exposed to a flame from underneath.	$x = 0.345 \frac{t^{1.3}}{\rho - \rho_c}$ where x = location of char front, mm; t = time, min; ρ = relative density of wood; ρ_c = relative density of char.
Schaffer I (ASTM E 119 fire exposure)[13] Douglas-fir laminated to 75 mm thick planks and exposed to ASTM E 119; moisture content ranged from 6% to 18%. Similar equations are available for southern pine and white oak.	$t = [(2.27 + 0.046\omega)\rho + 0.33]x$ where x = location of char front, mm; t = time, min; ρ = relative density of wood; ω = moisture content of wood, %.
Schaffer II (constant-temperature exposure)[13] Douglas-fir laminated to 3 inch thick planks and exposed to constant furnace temperatures of 538°, 816°, 927°C from one side; moisture content ranged from 6% to 18%. Similar equations are available for southern pine and white oak.	$t = -k \ln\left\{1 - \frac{x}{3.0}\right\} \exp\left\{\frac{JE}{RT}\right\}$ where $k = (28.576 + 0.576\omega)\,\rho + 4.548$; T = temperature, K; J = 4.184 joules/cal; R = 8.14 joules/(gram-mole·K); E = 3108 cal/gram-mole; x = location of char front, inch; t = time, min; ρ = relative density of wood; ω = moisture content of wood, %.
White[14,15] 63 mm thick specimens from eight species exposed to ASTM E 119; moisture content ranged from 6% to 16%.	$t = kx^{1.23}$ where $\ln(k) = -1.7418 + 0.8485 f_c + 0.9388\rho + 0.02\omega$; f_c = char contraction factor, dimensionless; ρ = relative density of wood; ω = moisture content of wood, %; x = location of char front, mm

and a coefficient of variation of 7.6%. The average fractional moisture content of the oven-dry weight was 0.093 with a coefficient of variation of 3.1%.

Image analysis

Each of the retained sections of the exposed specimens was cleaned with a metal scraper to remove char particles. Then an image of the cross sectional area of the sample was captured using a microprocessor-based imaging system. Examples of such images are shown in Fig 1. The area was computed using software provided with the imaging system. This value is an estimate of the residual area (A) with a duration of exposure t approximately equal to the time to failure of the specimen. Five specimens were excluded from this analysis because of missing data. A total of 55 values of A were obtained.

The images shown in Fig. 1 are typical of residual areas of specimens at various times to failure. As expected, the residual area retained, approximately, a rectangular shape throughout the exposure period but the comers became progressively more rounded. With the exception of the charring at the comers, the depth of char appears to be more or less uniform between the narrow and the wide faces. Charring can, however, be retarded by the presence of a knot because density of knot-wood is generally higher than that of normal wood (see image 863 in Fig 1). Little quantitative work has been done on the effect of knots on charring rate. It should be noted that these charring irregularities will preclude any sensible measurement of the rate of charring in such regions. An 'apparent' rate will need to be developed to incorporate the effects due to knots. It is suspected that in wood containing edge knots, the loss of load-carrying capacity due to charring may be insignificant compared with the loss due to elevated temperatures near charring, particularly when it is under tension, because of the development of shrinkage cracks. In members subjected to eccentric loading in compression, the charring behaviour near knots may be conveniently neglected because the probability that a 'worst' knot defect also occurs in the same location as the maximum stress is relatively low.

MODELLING APPROACH

The residual area A is plotted against *t* in Fig 2, which indicates that a linear-regression model can be

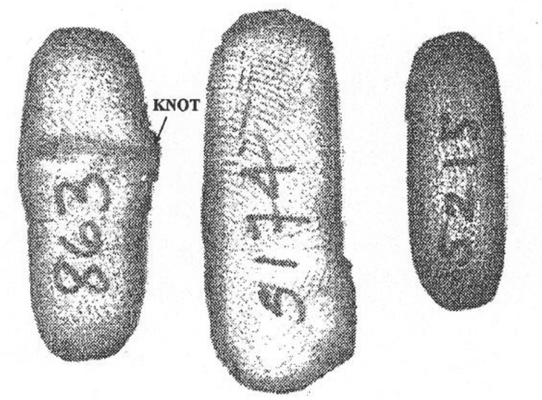

Figure 1. Typical images of residual areas as captured using a computer-based imaging system.

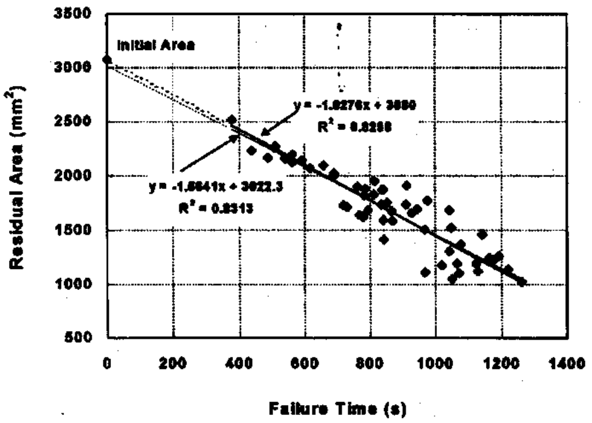

Figure 2. Residual areas versus time of exposure.

reasonably fitted to these data. The data subject to the linear regression were the residual areas as determined, from which we obtain:

$$A(t) = -1.564\,t + 3022.3. \tag{4}$$

The average rate of change of the residual cross-sectional area has been estimated from the slope of the fitted regression line, which in turn provides the basis for the derivation of the dimensional rate of charring along the major or minor axis. The regression is shown in Fig. 2 as a light line along with the data. Using this relationship, the 'average' rate of change of the residual area is predicted to be - 1.564 mm^2/s. In addition, the initial area is predicted to be 3022.3 mm^2, as given by the intercept of the equation. Because this value does not differ 'significantly' from the original area of 3080 mm^2 (35 mm × 88 mm) the regression model was modified by forcing the line through the point of 3080 mm^2 at time 0, yielding

$$A(t) = -1.628\,t + 3080. \tag{5}$$

This second line is shown in Fig. 2 as a darker line. The slope of the line is - 1.628 mm^2/s which represents the rate of reduction of the cross-sectional area from the initial area of 3080 mm^2. This slope is the area charring rate (cc).

Norén's char data, shown in Fig. 7b, also appear to be linearly related to the time of exposure. However, if the trend line through his data is extended back to time zero, the line would have to curve down in order to intercept the initial area at time zero. This behaviour was caused by the ISO 834 fire exposure (which is quite similar to ASTM E 119) which initially starts off at room temperature and only reaches 539°C at 5 min. Our exposure was a constant temperature of 500°C.

Dimensional charring rate

The dimensional charring rate (β) is determined by assuming that the thicknesses of char in the direction along the major and the minor cross-sectional dimensions are the same. At any time t, the residual cross-sectional area $A(t)$ is given by

$$A(t) = a(t)b(t) \tag{6}$$

where $a(t)$ and $b(r)$ are the residual cross-sectional dimensions at time t. Furthermore,

$$a(t) = a_0 - 2\delta(t) \tag{7}$$

and

$$b(t) = b_0 - 2\delta(t) \tag{8}$$

where a_o and b_o are the initial uncharred cross-sectional dimensions and $\delta(t)$ is the total depth of char measured from one side as a function oft. Taking the derivatives of Eqns (6), (7) and (8), we obtain, respectively

$$\frac{\partial A(t)}{\partial t} = \frac{\partial b(t)}{\partial t} a(t) + \frac{\partial a(t)}{\partial t} b(t) \tag{9}$$

$$\frac{\partial a(t)}{\partial t} = -2\frac{\partial \delta(t)}{\partial t} \tag{10}$$

$$\frac{\partial b(t)}{\partial t} = -2\frac{\partial \delta(t)}{\partial t}. \tag{11}$$

Substituting Eqns (10) and (11) into (9), and letting $\partial A(t)/\partial t = \alpha$, yields

$$\frac{\partial \delta(t)}{\partial t} = \beta(t) = \frac{\alpha}{-2a_0 - 2b_0 + 8\delta(t)} \tag{12}$$

where $\partial\delta(t)/\partial t = \beta(t)$ is the instantaneous dimensional charring rate in the transverse direction at time t. Solving this first-order differential equation, we obtain

$$\frac{\partial \delta(t)}{\partial t} = \beta(t) = -\frac{\alpha}{8}\left[\frac{\alpha t}{4} + \frac{1}{16}(a_0 + b_0)^2\right]^{-1/2} \tag{13}$$

$$\delta(t) = \frac{1}{4}(a_0 + b_0) - \left[\frac{\alpha t}{4} + \frac{1}{16}(a_0 + b_0)^2\right]^{-1/2}. \tag{14}$$

Eqns (13) and (14) give the dimensional charring rate and char depth expressed as a function of t, the initial cross-sectional dimensions a_0 and b_0 and α. The dimensional charring rate is shown in Fig. 3 with a_0 = 35 mm, b_0 = 88 mm and α = - 1.628 mm^2/s. From Fig. 3, the charring rate is predicted to increase gradually over time, from 0.397 mm/min at t = 0 s to 0.524 mm/min at t = 1000 s. The average charring rate over that period is

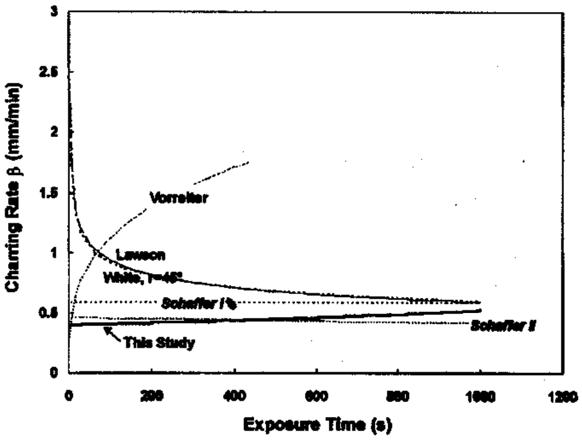

Figure 3. Dimensional charring rates (β) of wood exposed to elevated temperatures.

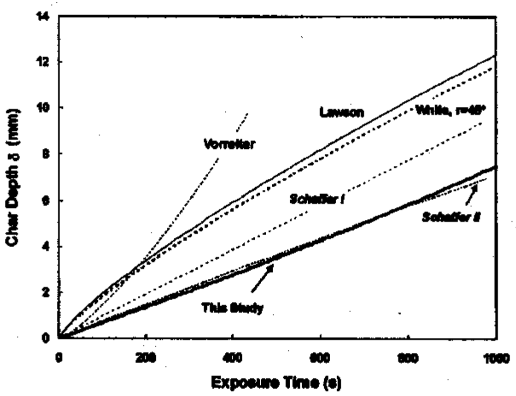

Figure 4. Depth of char (δ) of wood exposed to elevated temperatures.

calculated to be 0.451 mm/min. Compared with the rate of 0.6mm/mm for large-section timber exposed to ASTM E 119 exposure, this value is reasonably lower because the exposure temperature used in this study was only 500°C. The ASTM time curve has the following temperatures: 539°C at 5 min; 704° at 10 min; 843° at 30 min; and 927° at 60 min.

Figure 3 also shows the prediction curves of Lawson, Vorreiter, Schaffer, and White, whose models are de scribed in Table 1. The char depths (δ) calculated as a function of time on the basis of these models are compared in Fig. 4. In general, the rates predicted by these models depend significantly on the exposure conditions. Some of the observed differences are species, moisture content and size effects, some are attributable to limitations associated with the models. Models developed by Lawson or Vorreiter were not intended to be used to predict the rate of charring at the initial stage of exposure. Those predictions, and therefore their differences at the initial stage of exposure (see Fig 3), are the result of the model choices used rather than of the actual phenomena.

It is noted that our results and *Schaffer II* (with $T = 500 + 273$ K) on δ are similar. *Schaffer II* was developed for constant-temperature exposure based on 75-mm-thick Douglas-fir planks exposed to one side. While the two models predict almost the same char depth up to 1000 s (see Fig. 4), our model predicts that the dimensional charring rate β is to increase gradually over time whereas *Schaffer II* predicts that it is to decrease gradually. This difference can be attributable to the fact that Schaffer's exposure was from one side only. Both studies suggest that the use of a single charring rate for design purposes may not be appropriate.

VARIABILITY OF CHARRING RATES

In designs based on probabilistic theory where the objective is to limit the probability of failure with respect to the performance function, variability of the design parameters is an important design input. The rate of charring is an important design parameter but is also high in variability as can be observed in the rate of charring among the 55 specimens exposed (see Fig. 2). In these tests, all we know is that the charring history of an individual specimen had to pass through two known points—one at the beginning of the exposure and the other at the end of the exposure. Assuming that individual behaviour is also a linear function oft, the slope. of the line joining the two known points is the best estimate of this rate. The variability can then be evaluated by examining the distributional characteristics of these slopes.

The results of this examination are plotted in Fig 5 as a cumulative frequency distribution. The *Normal, Weibull* and *Lognormal* distribution models were fitted to the frequency distribution data The *Lognormal* model provides the best 'fit' to the data. According to Bury[18], *Lognormal* is an appropriate model for a measurable characteristic whose underlying causes are numerous, independent of each other, and whose 'sum' effect is 'multiplicative'. The charring variable indeed possesses these characteristics since variability in charring occurs naturally as a result of many factors, including, mostly, differences in material properties-between specimens and within a specimen-such as density, moisture content, permeability, and lignin content.[14] Among these factors, moisture content and density are most important. Variability can also be caused by external factors such as variability of furnace temperature. These factors are largely independent of each other. Furthermore, there is evidence found in the models of White[14] and Schaffer[13] to suggest that the combined effect of these factors is multiplicative. For instance, White's charring model implies a multiplicative effect due to char contraction factor (f_c), density (ρ) and moisture content (ω). His charring model relates time t to the location of char front x by

$$t = mx^b \tag{15}$$

where m is given by

$$\ln(m) = -1.7418 + 0.8485 f_c + 0.9388 \rho + 0.0197 \omega. \tag{16}$$

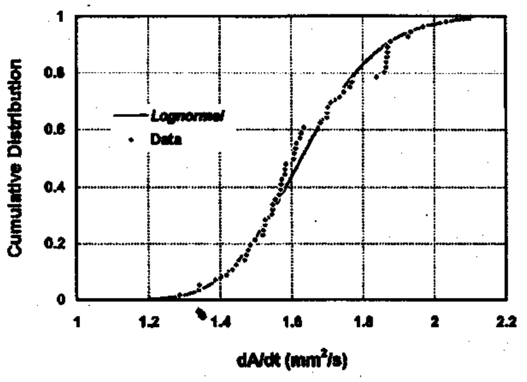

Figure 5. Cumulative frequency distribution of residual charring rates.

Differentiating x of Eqn (15) with respect to t, we obtain

$$\frac{\partial x}{\partial t} = \beta = m^{-1/b} b^{-1} t^{(1/b)-1} \quad (17)$$

where

$$m = e^{-1.7418} e^{0.8485 f_c} e^{0.9388\rho} e^{0.0197\omega}. \quad (18)$$

It is obvious from Eqn (17) and Eqn (18) that the sum effect of f_c, ρ and w on β is multiplicative.

Lognormal distribution

The distribution of charring rate of the basis of residual area (let $\alpha = \partial A/\partial t$) is given by the *Lognormal* distribution

$$F_{LN}(\alpha; \mu, \sigma) = \frac{1}{\sigma\sqrt{2\pi}} \int_0^{\alpha} \frac{1}{\alpha} \exp\left\{-\frac{1}{2}\left(\frac{\ln\alpha - \mu}{\sigma}\right)^2\right\} d\alpha \quad (19)$$

where F_{LN} is the cumulative frequency, ($\sigma = 0.106$, and $\mu = 0.486$. This function can be used to generate the random value of the area charring rate for reliability analysis.

VARIABLE-TEMPERATURE EXPOSURES

In order that the area-charring model can be used for design purposes or for reliability analysis, it should be extended to predict charring behaviour under other constant temperatures or variable temperatures. Obtaining data for these extensions experimentally would he costly. Instead, we used *Schaffer II* (Table 1) to calibrate a function for α, such that $\alpha(T) = a(T - T_c)^b$, where T is the temperature of exposure and T_c is the temperature of charring Since *Schaffer II* is almost identical to ours in its predictions of δ over a period of 1000 s at $T = 500°C$ (see Fig 4), we reasoned that *Schaffer II* can be used to provide the 'shift' needed in α for other constant temperatures of exposure while the fundamental characteristic of our model, that the area charring rate is constant for a given constant temperature of exposure, is maintained. This approach incorporates T into the area-charring model as an independent variable.

The procedure to determine the α for other temperatures of exposure is as follows: First, a set of d values (δ_i, t_i) at several selected times t within the 1000 s time span was generated using *Schaffer II* for each exposure temperature of 500°, 600°, 700°, etc., up to 1000°C. The set of δ values for each of these exposure temperatures is then substituted into Eqn (14) to compute a corresponding set of α values. The mean of the set was then determined, which was assumed to be the area charring rate for the temperature of exposure (a(T)). Then for $T > T_c = 288°C$, we let

$$\alpha(T) = a(T - T_c)^b. \quad (20)$$

The values of the coefficients a and b are then determined by least-square regression. For $T < T_c = 288°C$, $\alpha(T)$ was assumed to be zero.

Note that Eqn (20) may be integrated to predict the residual area of lumber exposed either to constant-temperatures or to variable-temperature histories such as ASTM E 119. Note also that the coefficients a and b depend on size because Eqn (14) is size dependent, and on moisture content and relative density of wood because *Schaffer II* is moisture-content and density specific. Figure 6 shows area charring rates predicted as a function of T (constant-temperature) for a 35 × 88 mm² lumber member with a moisture content ω = 9% and relative density ρ = 0.51. Coefficients a and b for lumber sizes of *2 × 4, 2 × 6,* and *2 × 8,* moisture contents of 8% and 12%, and relative density of 0.40, 0.45 and 0.50, have been determined and are tabulated in Table 2.

Model testing

Equation (20) was evaluated baaed on two sets of data found in the literature: (1) Norén's ISO 834 data on spruce[16] with an initial moisture content of 18.6% and a relative density of 0.47, and (2) Schaffer's ASTM E 119 data on Douglas-fir with an initial average moisture content of 7.3% and a relative density of 0.48. The coefficients a and b were determined for each case as described previously for the initial cross-sectional dimensions of $a_0 = 45$ mm and $b_0 = 120$ mm in the case of Norén, and

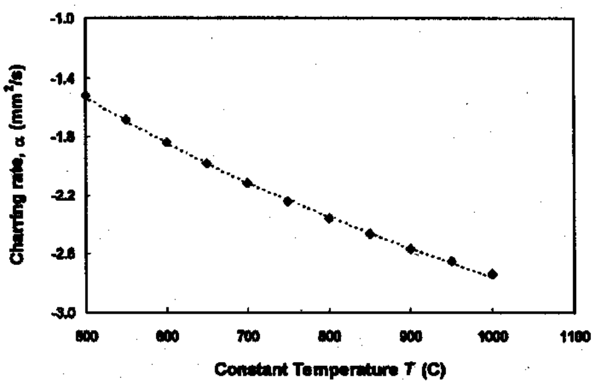

Figure 6. Area charring rate calibrated using Schaffer II (Table I).

Table 2. Coefficients *a* and *b*

Density ρ (oven-dry)	Moisture content ω (%)	Lumber cross-sectional dimension (mm) 38 × 89		38 × 140		38 × 191	
		a	*b*	*a*	*b*	*a*	*b*
0.40	8	−0.171	0.448	−0.179	0.509	−0.201	0.539
	12	−0.154	0.460	−0.164	0.517	−0.185	0.545
0.45	8	−0.142	0.469	−0.154	0.523	−0.174	0.551
	12	−0.128	0.480	−0.141	0.532	−0.160	0.557
0.50	8	−0.121	0.486	−0.134	0.536	−0.153	0.561
	12	−0.109	0.497	−0.122	0.544	−0.141	0.567

46.8 mm and 90.5 mm in the case of Schaffer. We obtained, for $T > T_c = 288°C$, $a = -0.11145$ and $b = 0.54$ for Norén. The respective values for Schaffer, are $a = -0.13079$ and $b = 0.49304$.

Then, replacing T with $T(t)$, the ISO 834 temperature-time curve, in Eqn (20), where

$$T(t) = T_0 + 345\log_{10}(8t+1) \quad (21)$$

and separating the variables by A and t, then performing an integration with respect to the variable on each side of Eqn (20), we obtain

$$\int_{A_0}^{A_R} dA = \int_{t_0}^{t_R} a(345\log_{10}(8t+1) + T_0 - T_c)^b dt. \quad (22)$$

The residual area A_R at time t_R is given by

$$A_R = A_0 + \int_{t_c}^{t_R} a(345\log_{10}(8t+1) + T_0 - T_c)^b dt \quad (23)$$

where t_c is the time it takes to reach the temperature. of T_c (which can be computed from Eqn (21)). In the case of Schaffer, the temperature curve was assumed to be also given by Eqn (21).

The results of this calculation and the two sets of experimental data are shown in Fig. 7. As shown in Fig. 7a, Schaffer's *2 × 4* data are reasonably predicted, while those of Norén (Fig. 7b) are over-predicted. The over-prediction is probably the result of a significant difference in permeability between the spruce Norén used and the Douglas-fir used in Schaffer's experiment in developing this second model. Because the moisture content of Nor&n's data was high—18.6%—permeability probably played a significantly greater role in affecting the rate of charring.

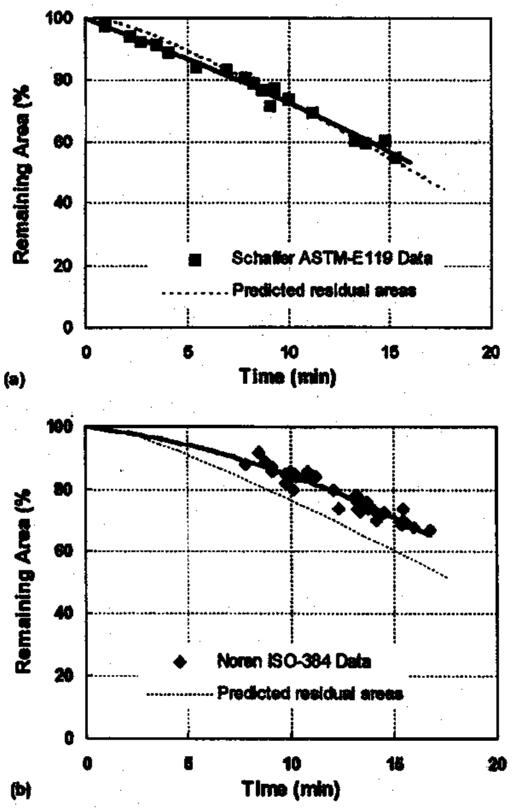

Figure 7. Model predictions of Schaffer's ASTM E 119 Douglas-fir data (a) and Norén's ISO 834 spruce data (b).

CONCLUSIONS AND RECOMMENDATIONS

This paper reports the charring behaviour of 55 specimens of *2 × 4* SPF lumber exposed to 500°C in a furnace. A linear model of the residual area was developed yielding a constant rate of charring of 1.628 mm^2/s. The corresponding 'dimension' charring rate is found to be a function of time with an average value of approximately 0.45 mm/min (0.0075 mm/s). The rate is predicted to increase gradually with time of exposure, to a value of 0.52 mm/min at an exposure time of 16min. These dimensional charring rates are reasonably consistent with the results of several other experiments reported in the literature. Finally, the variability of the area charring rate among the specimens tested can be characterized by a *Lognormal* distribution. The distribution can be used as an input to reliability analysis of a structural member exposed to a 500°C environment by treating the residual cross-sectional area as a variable.

An area-charring model which incorporates an existing model by Schaffer[13] to express the rate of charring as a function of temperature of exposure, has been developed to predict residual areas of lumber exposed to constant-temperature or variable-temperature histories. This empirical approach was found to predict, with reasonable accuracy, a sample of 45 × 120 mm^2 spruce lumber exposed to ISO 834 fire exposure. This model is capable of predicting char depth as a function of time given a variable-temperature. history. It is recommended that this model be improved to account for the permeability effect in wood with high moisture contents.

Acknowledgment

Forintek Canada Corp. would like to thank its industry members, Natural Resources Canada (Canadian Forest Services), and the Province of British Columbia, Alberta, Québec, Nova Scotia and New Brunswick, for their guidance and financial support for this research.

REFERENCES

1. Lau PWC, Barrett D. Modelling the reliability of wood tension members exposed to elevated temperatures. *Wood Fiber Sci.*, July 1998.
2. ASTM E 119-95a, *Standard Method of Fire Endurance Tests of Building Construction and Materials.* American Society for Testing and Materials: Philadelphia, PA, 1995.
3. CAN/ULC-S101-M89, *Standard Method of Fire Endurance Tests of Building Construction and Materials.* Underwriters' Laboratories of Canada: Scarborough, Ontario, Canada, 1989.
4. ISO 834, *Fire-Resistance Tests—Elements of Building Construction.* International Standards Organization: Geneva, Switzerland, 1975.
5. Lee TT. A method for assessing the fire resistance of laminated timber beams and columns. *Can. J. Civil Eng.* 1977; **4**: 161–169.
6. Hay R. Fire damage sensitivity criteria for wood fibre structures: Proposal for a new international standard. *Proceedings of 1990 International Timber Engineering Conference,* ed. by Hideo Sugiyama, Science University of Tokyo, Japan, Vol. 1, 100–109, 1990.
7. König J. Modelling the effective cross section of timber frame members exposed to fire. Paper presented at 1991 *Meeting of the International Council for Building Research Studies and Documentation,* Working Commission W18A-Timber Structures, 1991.
8. Jean M. The behaviour in fire of wood and wood-based materials. *Presented at the IUFRO Fifth-Conference on Wood Technology.* US Forest Products Laboratory, Madison, WI 1963.
9. Lawson DI, Webster CT, Ashton LA. Fire endurance of timber beams and floors. *J. Struct. Eng.* 1952; **30**(2): 27–34.
10. Truax TR. Fire research and results at US Forest Products Laboratory. *United States Forest Service Research Report No. 1999,* Madison, WI, 1959.
11. Blackshear PL, Jr., Murty KA, *The Measurement of Physicochemically Controlled Ablation Rates.* Tech. Rep. No. 1 (AD 285 460). University of Minneapolis Institute of Technology, Minneapolis, 1962.
12. Vorreiter L. Combustion and heat insulating losses of wood and fibreboards. *Holzforschung* 1956; **10**(3): 73–80.
13. Schaffer EL. Charring rate of selected woods transverse to grain. *United States Forest Service Research Paper FPL 69,* Forest Products Laboratory, Madison, WI, 1967.
14. White RH. *Charring Rates of Different Woods Species,* PhD dissertation, University of Wisconsin, Madison, WI, 1988.
15. White RH, Nordheim EV. Charring rates of wood for ASTM E119 exposure. *Fire Technology,* February 1992.
16. Norén JB. Failure of structural lumber when exposed to fire. In *Proceedings* 1988 *International Conference on Timber Engineering,* ed. by R. Y. Itani, pp. 397–406, Washington State University.
17. Schaffer EL. *The Effects of Fire on Selected Structural Timber Joints,* Master Thesis, University of Wisconsin, Madison WI, 1961.
18. Bury KV. *Statistical Models in Applied Science,* John Wiley & Sons: New York, 1975.

